forests

MDPI

Article

Soil Microbial Biomass and Community Composition across a Chronosequence of Chinese Cedar Plantations

Ya Shen †, Shichen Xiong †, Chengming You, Li Zhang, Yu Li, Zongwen Hong, Yifan Hu, Jing Li, Han Li, Lixia Wang, Sining Liu, Bo Tan and Zhenfeng Xu *

National Forestry and Grassland Administration Key Laboratory of Forest Resources Conservation and Ecological Safety on the Upper Reaches of the Yangtze River, Forestry Ecological Engineering in the Upper Reaches of the Yangtze River Key Laboratory of Sichuan Province, Institute of Ecology and Forestry, Sichuan Agricultural University, Chengdu 611130, China

* Correspondence: xuzf@sicau.edu.cn

† These authors contributed equally to this work.

Abstract: Afforestation is one of the most important forestry practices, but its impact on soil microbial communities remains poorly understood. In this study, we sampled the soil from 0–15 cm and 15–30 cm soil depths of 7-, 13-, 24-, 33-, and 53-year-old Chinese cedar (*Cryptomeria japonica var. sinensis*) plantations. To investigate the effect of stand age on soil microbial communities and their potential drivers, we measured phospholipid fatty acids (PLFAs) and soil physicochemical properties. At the 0–15 cm soil depth, the biomass of total PLFAs and functional microbial groups such as bacteria (B), fungi (F), Gram-negative bacteria (GN), Gram-positive bacteria (GP), actinomycetes (ACT), and arbuscular mycorrhizal fungi (AMF) increased sharply in 7- to 13-year-old stands, but then gradually leveled off in older stands. On the other hand, the biomass of total PLFAs and functional microbial groups at the 15–30 cm soil depth peaked in the 33-year-old stand. The biomass of total PLFAs and functional microbial groups was strongly influenced by stand age and soil depth, and was significantly lower at the 15–30 cm soil depth than at the 0–15 cm soil depth except for the 7-year-old stand. The F/B and fungi/total PLFAs ratios of both soil depths were markedly lower in the 13-year-old stand than in the remaining four stand ages, while the proportions of the bacterial group (GP and GN) showed contrasting trends. The biomass of all functional microbial groups and the GP/GN ratio were mainly mediated by soil organic carbon (SOC) concentration and the soil organic carbon to total phosphorus (C/P) ratio at the 0–15 cm soil depth, but primarily affected by ammonium nitrogen (NH_4^+-N) concentration at the 15–30 cm soil depth. The F/B ratio of the two soil depths was prominently affected by nitrate nitrogen (NO_3^--N) concentration. Our results highlighted that SOC concentration and mineral N (i.e., NH_4^+-N and NO_3^--N) concentration mainly drove changes in the soil microbial biomass and community composition with stand age in Chinese cedar plantations, and that the 13-year-old stand may be the key period for management.

Keywords: stand age; phospholipid fatty acid; soil microbial community; *Cryptomeria japonica var. sinensis* plantations

Citation: Shen, Y.; Xiong, S.; You, C.; Zhang, L.; Li, Y.; Hong, Z.; Hu, Y.; Li, J.; Li, H.; Wang, L.; et al. Soil Microbial Biomass and Community Composition across a Chronosequence of Chinese Cedar Plantations. *Forests* **2023**, *14*, 470. https://doi.org/10.3390/f14030470

Academic Editors: Anita J. Antoninka and Kara Gibson

Received: 1 January 2023
Revised: 18 February 2023
Accepted: 23 February 2023
Published: 24 February 2023

1. Introduction

The role of soil microorganisms in preserving biogeochemical cycles and soil fertility balance cannot be overemphasized and has been extensively studied in various ecosystems, especially in agroecosystems and forest ecosystems [1–3]. Unlike agroecosystems, forests do not rely on external factors such as fertilization to support tree growth, but instead primarily rely on microbial-mediated internal processes such as nutrient mineralization and litter decomposition [4,5]. The productivity of forests may be significantly affected by changes in soil microbial communities [6]. The world's planted forest area increased by more than 105 million ha between 1990 and 2015, accounting for seven percent of the global

forest area reported in 2015 [7]. Therefore, increasingly deeper insights into soil microbial communities following afforestation are important in assessing soil quality, maintaining soil fertility, and ensuring sustainable management of plantation ecosystems.

Forest age has wide implications for soil microbial communities [8]. First, stand age can regulate the input of organic matter (such as litterfall and root exudates) to the soil in the forest ecosystems and thus affect the food source (carbon source) of soil microorganisms [9,10]. Second, forest age can also affect the habitat of soil microorganisms by adjusting the understory vegetation and soil physiochemical properties, which then affect the biomass and community composition of soil microorganisms [11,12]. In addition, nutrient uptake strategies and plant growth rates vary with forest age, resulting in the functional microbial populations competing for nutrients and altering the soil microbial community composition [13,14]. Although more and more attention has been paid to the influence of forest age on soil microorganisms in plantation forests in recent years, the results of various studies remain controversial due to differences in stand age sequence and tree species selection.

Studies have shown that soil microbial communities are strongly correlated with soil physicochemical properties [15]. For example, soil physical properties (e.g., water content, soil bulk density, soil aggregate formation, and total porosity) significantly affected the microbial activity and composition of soils [16,17]. Soil pH correlated positively with microbial biomass and community composition, with bacterial communities sensing small changes in soil pH better than fungi [18,19]. Changes in soil organic matter and nutrient availability (e.g., ammonium nitrogen (NH_4^+-N) and nitrate nitrogen (NO_3^--N)) can alter microbial communities, particularly bacterial and fungal communities [19,20]. The relationship between soil microorganisms and soil physicochemical properties can also be expected to vary with stand age. Wang et al. [21] reported that microorganisms are sensitive to the dynamics of soil organic carbon (SOC) with stand age. Soil moisture, water holding capacity, SOC concentration, pH, and nutrient concentration play important roles in determining soil microbial biomass and community composition along an age gradient [10,12]. However, the relationship between soil properties of different forest ages and microbial communities in plantation forest ecosystems is not fully understood. In addition, the response of soil microbial communities to stand age may vary with soil depth because different soil depths receive different nutrient inputs [5,22,23]. Therefore, it is unclear whether the soil microbial communities and their main drivers differ by soil depth in the context of forest age sequences.

Southwestern China's ecological development depends greatly on the Chinese cedar (*Cryptomeria japonica var. sinensis*), which plays a major role in afforestation [24]. However, the soil fertility of Chinese cedar plantations has significantly declined in recent years, and the ecological and economic benefits are difficult to achieve [25]. This study investigated soil microbial communities from 0–15 and 15–30 cm soil depths in 7-, 13-, 24-, 33-, and 53-year-old Chinese cedar plantations. We hypothesized that (i) microbial communities would vary with stand age at both soil depths due to an increasing input of fresh organic matter to the forest floor [23], and (ii) SOC and NH_4^+-N would contribute most to the changes in the soil microbial communities at both soil depths with stand age because SOC is a critical driver of microbial communities and NH_4^+-N is one of the primary forms of N used for microbial protein synthesis [19,26]. Our study aims to investigate the changes and mechanisms in the soil microbial biomass and community composition along a chronosequence of Chinese cedar plantations.

2. Materials and Methods

2.1. Site Description

This research was carried out at the Sichuan Agricultural University's Long-Term Artificial Forest Ecosystems Station (29°24′–30°00′ N, 102°49′–103°32′ E), which is situated at the Hongya county state-owned forest farm on the western edge of the Sichuan Basin in China. The study area belongs to the subtropical humid zone. The average annual

precipitation was about 1600 mm, with an average annual temperature of 16.8–17.2 °C. The annual mean relative humidity was 79%–81%, and the annual sunshine hours were low (894–2054 h) (Table S1, http://data.cma.cn (accessed on 5 December 2022)). According to the FAO, the major soil type is classified as mountain yellow soil [7]. The total area of plantation in Hongya Forest Farm is about 11,370 ha, of which Chinese cedar (*Cryptomeria japonica var. sinensis*) accounts for 49.6% of the total area. Chinese cedar plantations have a complete age gradient from young forest to mature forest. The understory vegetation mainly includes *Fargesia spathacea*, *Rubus swinhoei*, *Elatostema involucratum*, *Pteridophyta*, etc. [27].

2.2. Experimental Design

The Chinese cedar plantations of different stand ages (7, 13, 24, 33, and 53 years old) were selected as the research objects in July 2021. The five stand ages are divided into young (7 years old), middle-aged (13 years old), near-mature (24 years old), mature (33 years old), and over-mature forest (53 years old) according to forestry industry standards. Young forests were established by planting 2-year-old Chinese cedar seedlings on sites that had undergone a short period of recuperation after the over-mature forests had been clear-cut. As the tree grows, the following practices are taken: weeding twice a year for the first three years to promote the growth of the seedlings, and then avoiding frequent management until harvest. The areas of young, middle-aged, near-mature, mature, and over-mature forests are 2134 ha, 698 ha, 577 ha, 866 ha, and 1790 ha, respectively [17]. In this study, three plots with an area of 20 m × 20 m were set in each forest age, and the distance between plots was more than 100 m. Each plot was measured for canopy density, diameter at breast height (DBH, 1.3 m), and tree height. The basic conditions of the Chinese cedar plantations with different forest ages were given in Table S2.

2.3. Soil Sampling

To facilitate the comparison of soil microbial communities among different stand ages, the sampling depth was unified, and the litter layer was removed from each plot before soil collection. According to the five-point sampling method, 5 soil cores from each plot were obtained using a stainless-steel cylinder (diameter 5 cm) at soil depths of 0–15 cm and 15–30 cm, and then the soil cores with the same depth were mixed into a composite sample. A total of 30 composite samples (5 stand ages × 3 plots × 2 soil depths) were collected. The soil samples were packed in cooler boxes with ice packs, transported to the laboratory within 24 h, and sifted with a 2 mm mesh. These samples were temporarily kept at 4 °C in a refrigerator to facilitate dispensing and the measurement of several indicators that call for fresh samples. A portion of the dispensed sample was air-dried for routine indicators (e.g., pH, soil organic carbon (SOC) concentration, total phosphorus (TP) concentration, and total nitrogen (TN) concentration), while another portion was freeze-dried for PLFA analysis. Table S3 displays the physicochemical properties of the soil at various stand ages.

2.4. Soil Physicochemical Analysis

The soil bulk density (SBD) and gravimetric water content (GWC) were calculated by weighing fresh and oven-dried bulk soil cores. Soil pH was measured in the soil suspension (1:2.5 *w*/*v* air-dried soil to water) using a digital pH meter [28]. SOC concentration was measured by potassium dichromate oxidation titration. First, 5 mL of 0.8 M $K_2Cr_2O_7$ and 5 mL of H_2SO_4 were added to the soil, which was then boiled at 220 °C for 15 min. Titration with 0.2 M $FeSO_4$ was performed on the remaining $K_2Cr_2O_7$ [29]. TP and TN concentrations in soil were measured by molybdenum-antimony anti-colorimetry and Kjeldahl determination, respectively [27]. C/P, C/N, and N/P were calculated using the ratios of SOC to TP, SOC to TN, and TN to TP, respectively. Ammonium nitrogen (NH_4^+-N) and nitrate nitrogen (NO_3^-N) concentrations were extracted from 5 g of fresh soil with 2 M KCl solution, filtered through Whatman® qualitative filter papers, and determined by colorimetry (the indophenol blue method) and UV–visible spectrophotometry, respectively [27].

2.5. Phospholipid Fatty Acid (PLFA) Analysis

Using a buffer solution of chloroform, methanol, and phosphate (1:2:0.8 $v/v/v$), lipids were extracted from 4 g of freeze-dried soil. They were then separated into neutral lipids, glycolipids, and phospholipids on a 0.5 g silicic acid column (Supelco Inc., Bellefonte, PA, USA) by successively eluting them with chloroform, acetone, and methanol. Fatty acid methyl esters (FAME) were created by mild alkaline methanolysis of the phospholipids. The FAMEs were detected and quantified by using an Agilent 7890 B gas chromatograph (Agilent Technologies, Santa Clara, CA, USA) with identification software (MIDI Inc., Newark, DE, USA) and adding the methyl nonadecanoate (19:0, Sigma, St. Louis, MO, USA, CAS #1731-94-8, N5377-1G) as an internal standard [30]. Soil microbial biomass was calculated by summing the biomass for specific biomarkers and expressed as nmol PLFA nmol g^{-1} dry soil [1,31]. According to different signature fatty acids, several PLFA biomarkers for bacteria (B), Gram-negative bacteria (GN), Gram-positive bacteria (GP), fungi (F), arbuscular mycorrhizal fungi (AMF), and actinomycetes (ACT) were defined as described in Table 1. Total PLFAs were calculated as the sum of the functional microbial groups described in Table 1 together with 16:0 and 18:0. Additionally, the ratios of GP/GN and F/B are used as environmental indicators, indicating microbial stress and changes in habitat factors [18,32].

Table 1. Biomarker groups defined.

Biomarker Groups	Marker PLFA	References
Gram-positive bacteria	i15:0, a15:0, i16:0, i17:0, a17:0	[33,34]
Gram-negative bacteria	16:1ω7c, 16:1ω9c, 18:1ω7c, cy17:0, cy19:0	[33,34]
Bacteria	The sum of Gram-positive and Gram-negative biomarkers together with 15:0, 17:0	[31,35]
Fungi	18:1ω9c, 18:2ω6c, 18:3ω6c	[34,36]
Arbuscular mycorrhizal fungi	16:1ω5c	[31,37]
Actinomycetes	10Me16:0, 10Me17:0, 10Me18:0	[33,38]

2.6. Statistical Analysis

The Shapiro–Wilk test and the Levene test were used for data normality analysis and homogeneity of variance, respectively. To satisfy the ANOVA requirement, the soil physicochemical properties and the soil microbial biomass were logarithmically transformed, and the proportions of the functional group data were square root transformed. A two-way ANOVA was performed to investigate the impact of soil depth and stand age on soil microbial biomass, community composition, and soil physicochemical properties. Subsequently, a simple effect analysis (Bonferroni) was performed to assess the differences between five stand ages at the same soil depth or between soil depths at the same stand age when the interaction was significant. Moreover, differences in the proportion of functional groups between stand ages were determined by one-way ANOVA with post hoc Tukey tests. The aforementioned analysis was performed using SPSS software (SPSS version 27, IBM SPSS Inc., Chicago, IL, USA). We used all specific biomarker PLFAs to conduct a non-metric multidimensional scaling (NMDS) with the function "metaMDS", followed by an analysis of permutational multivariate analysis of variance (PERMANOVA) with the function "adonis2", utilizing the Bray–Curtis distance matrix to further clarify differences in soil microbial communities between stand ages or soil depths. The contribution of soil properties to the soil microbial communities was calculated using hierarchical partitioning through the "rdacca.hp" package [39]. Based on the results of the relative importance, the top three explanatory variables (soil physicochemical properties) of relative importance in each of the two soil depths were selected for correlation analysis with PLFAs. The physicochemical data were log-transformed, and then we employed the "ggpairs" function from the *GGally* package to generate scatter plots and calculate the Pearson correlation. The above analyses and graphics were performed using the "vegan", "GGally", and "ggplot2" packages in the R (version 4.2.0, R Core Team, 2022, Vienna, Austria) [40–42]. Column plots were generated using OriginPro 2022 (OriginLab Corporation, Northampton, MA, USA).

3. Results

3.1. PLFAs across Stand Ages

Stand age, soil depth, and their interaction had significant impacts on soil microbial biomass (Figure 1a–g). Specifically, the total PLFAs ranged from 5.8 to 25.0 nmol g^{-1} at the 0–15 cm soil depth across forest ages, with the 7-year-old stand having lower amounts than the remaining four stand ages. The total PLFAs of different stand ages at the 15–30 cm soil depth were 6.0–12.4 nmol g^{-1}, with a maximum in the 33-year-old stand (Figure 1a). Notably, PLFAs of functional microbial groups such as GP, GN, bacteria, fungi, AMF, and ACT showed similar patterns to the total PLFAs at both soil depths and were significantly lower at the 15–30 cm soil depth than at the 0–15 cm soil depth for all stand ages except for the 7-year-old stand (Figure 1b–g).

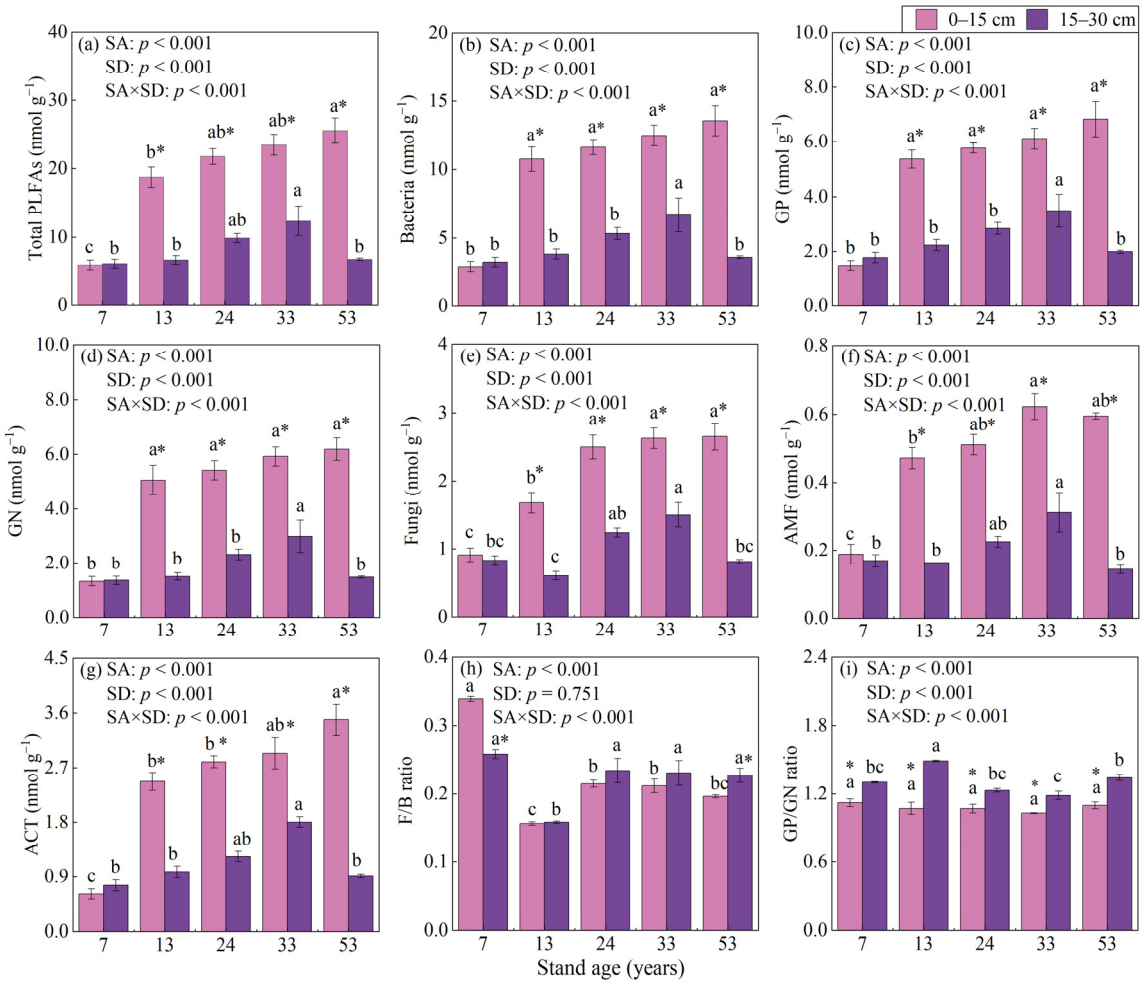

Figure 1. The biomass of (**a**) total phospholipid fatty acids (PLFAs), (**b**) bacteria (B), (**c**) Gram-positive bacteria (GP), (**d**) Gram-negative bacteria (GN), (**e**) fungi (F), (**f**) arbuscular mycorrhizal fungi (AMF), and (**g**) actinomycetes (ACT), (**h**) the F/B ratio, and (**i**) the GP/GN ratio from the 0–15 cm and 15–30 cm soil depths along the stand ages in the Chinese cedar plantations. Different lowercase letters denote statistically significant differences between forest ages at the same soil depth ($p < 0.05$). Significant changes between two soil depths of the same stand age are denoted by the asterisk ($p < 0.05$). Each sub-figure contains the results of a two-way ANOVA for the primary components (stand age (SA) and soil depth (SD)) and their interactions (SA × SD). Bonferroni was employed for main effect comparisons or post hoc analyses of simple effects. The bars show mean ± SE ($n = 3$).

The non-metric multidimensional scaling (NMDS) analysis of all specific biomarker PLFAs indicated that the soil microbial communities exhibited higher similarity in 24- and 33-year-old stands with the same soil depth, while there were distinct differences between

other forest ages or soil depths (Figure 2). Additionally, the permutational multivariate analysis of variance (PERMANOVA) analysis also indicated the soil microbial communities were substantially influenced by soil depth (R^2 = 0.361, $p < 0.001$), stand age (R^2 = 0.417, $p < 0.001$), and their interactions (R^2 = 0.153, $p < 0.001$) (Figure 2).

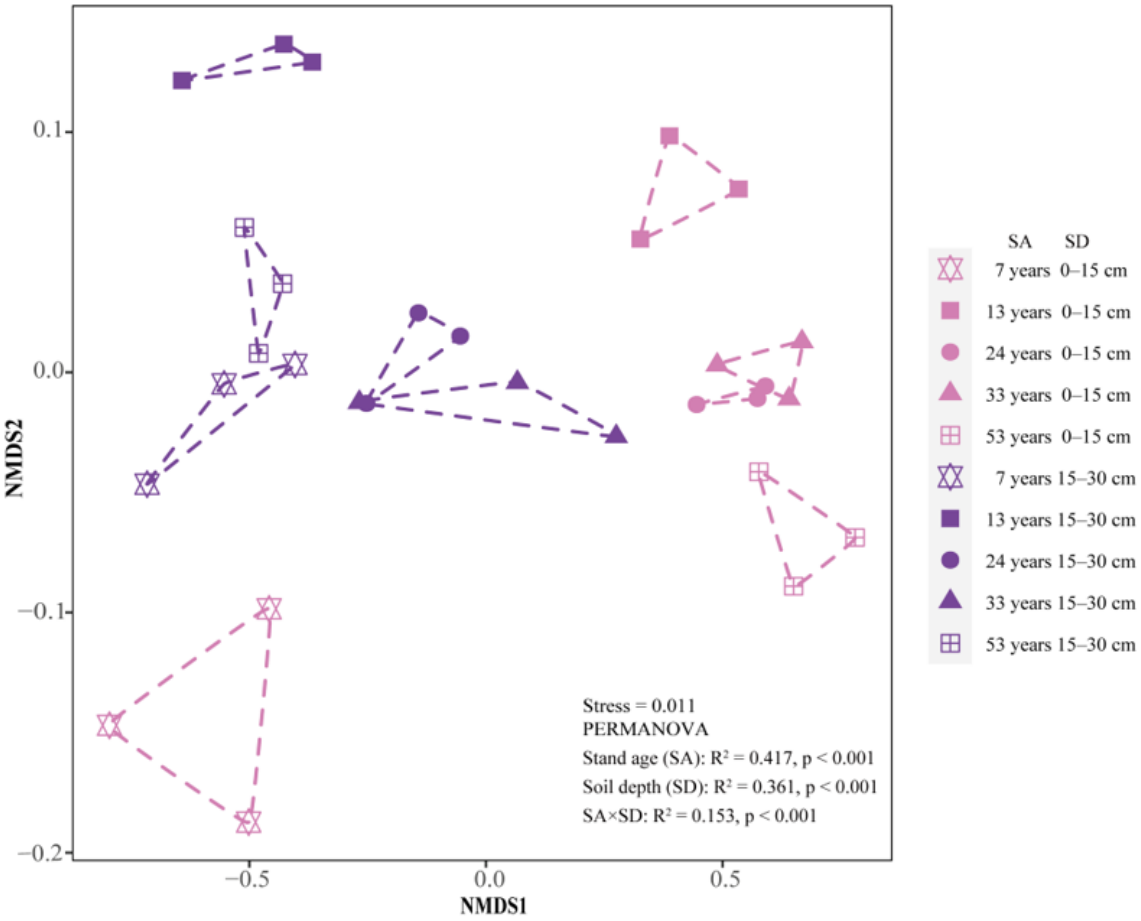

Figure 2. The results of non-metric multidimensional scaling (NMDS) and permutational multivariate analysis of variance (PERMANOVA) for all specific biomarker phospholipid fatty acids (PLFAs) are based on the Bray–Curtis distance matrix between different stand ages and soil depths. Colors and point shapes denote the soil depth (SD) and stand age (SA), respectively. The dashed line depicts the grouping of the samples based on the stand age.

3.2. Microbial Community Composition across Stand Ages

The soil microbial community composition was dominated by bacterial groups (GP and GN), followed by fungi and ACT at two soil depths of five stand ages (Figure 3a,b). Among them, the proportion of the bacterial groups was markedly higher in the 13-year-old stand than in the other four stand ages, while the proportion of the fungal group showed the opposite ($p < 0.05$) (Figure 3a,b). This result corresponded to the lowest F/B ratio of the 13-year-old stand and was mainly influenced by the stand age ($p < 0.001$) (Figure 1h). Concretely, at the 0–15 cm soil depth, the GP/total PLFAs, GN/total PLFAs, and ACT/total PLFAs significantly increased from 7- to 13-year-old stands and then stabilized, while the AMF/total PLFAs first decreased and then stabilized (Figure 3a). The GP/GN ratio and GP/total PLFAs were obviously higher in the 13-year-old stand than in other stand ages at the 15–30 cm soil depth ($p < 0.05$) (Figures 1i and 3b). The above results indicated that the composition of soil microorganisms changed markedly during the transition from 7- to 13-year-old stands (Figures 1h,i and 3). In addition, soil depth also significantly affected the GP/GN ratio, GP/total PLFAs, GN/total PLFAs, and AMF/total PLFAs ($p < 0.05$) (Figure 1i and Table S4). Specifically, the GP/GN ratio and GP/total PLFAs of

five stand ages were higher at the 15–30 cm than at the 0–15 cm soil depth, while there was an opposite trend for the GN/total PLFAs and AMF/total PLFAs (Figures 1i and 3).

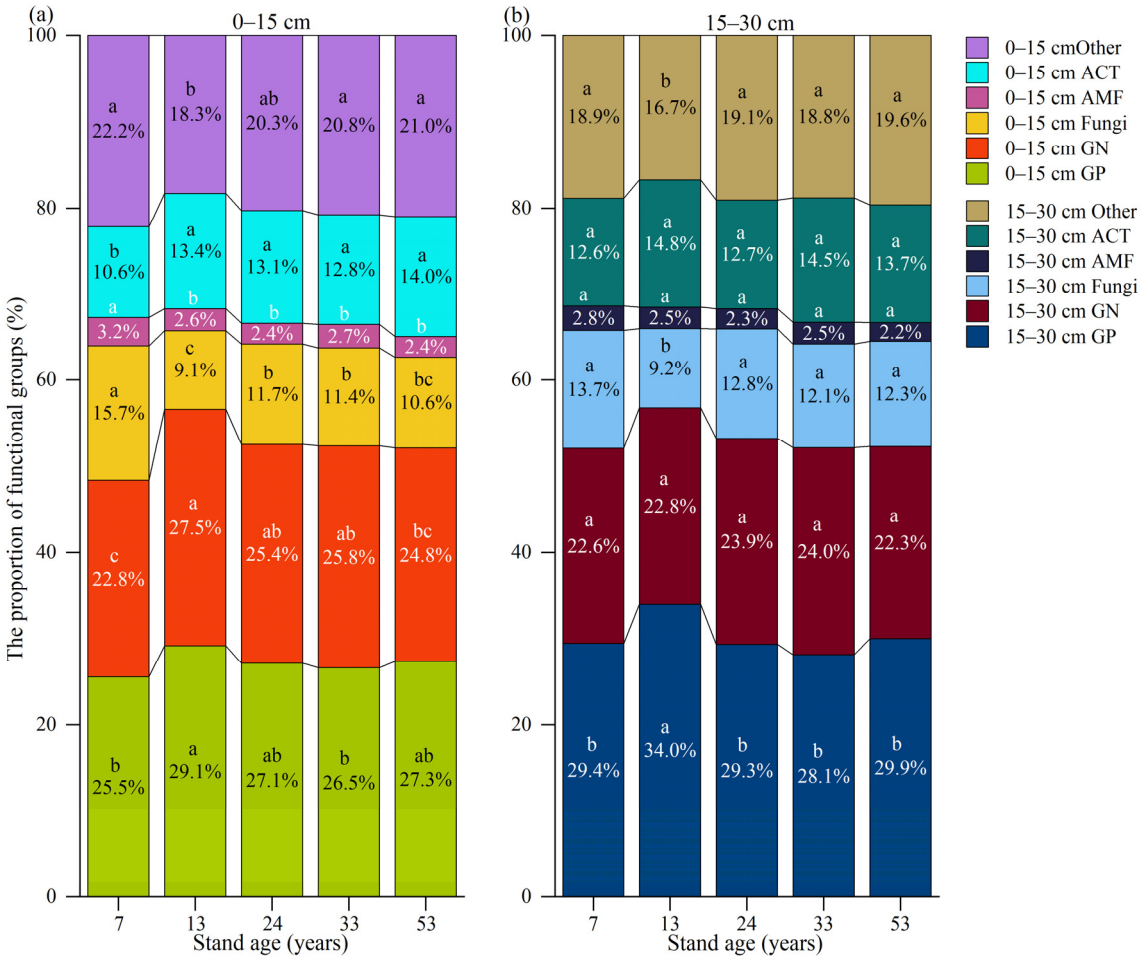

Figure 3. Changes in the proportion of functional groups from the (**a**) 0–15 cm and (**b**) 15–30 cm soil depths along the forest ages of the Chinese cedar plantations. Different lowercase letters indicate statistically significant differences between forest ages at the same soil depth. Abbreviations: sum of 16:0 and 18:0 (Other), arbuscular mycorrhizal fungi (AMF), actinomycetes (ACT), Gram-negative bacteria (GN), and Gram-positive bacteria (GP).

3.3. Contribution and Correlation Analysis of Soil Physicochemical Properties to Soil Microbial Communities

GWC, SOC concentration, N/P ratio, and nutrient concentrations, including TN, TP, and NH_4^+-N, increased and then decreased with increasing stand age at two soil depths, peaking in 24- or 33-year-old stands, while SBD showed the opposite trend. The variation patterns of C/N and C/P ratios and SOC concentration at the 15–30 cm soil depth were consistent, and there were no obvious variation patterns at the 0–15 cm soil depth. NO_3^--N increased significantly in 7- to 13-year-old stands but then flattened in 13- to 53-year-old stands. pH decreased from 7- to 24-year-old stands, then stabilized and differed significantly between the two soil depths (Table S3).

Hierarchical partitioning analysis showed that SOC concentration and C/P ratio were important factors influencing all microbial groups and the GP/GN ratio at the 0–15 cm soil depth, while NH_4^+-N concentration was the main factor regulating all microbial groups and the GP/GN ratio at the 15–30 cm soil depth (Figure 4). Interestingly, soil mineral nitrogen, including both NO_3^--N and NH_4^+-N, heavily affected the ratio of F/B at the 0–15 cm soil depth, while the F/B ratio at the 15–30 cm soil depth was mainly controlled by the NO_3^--N concentration (Figure 4).

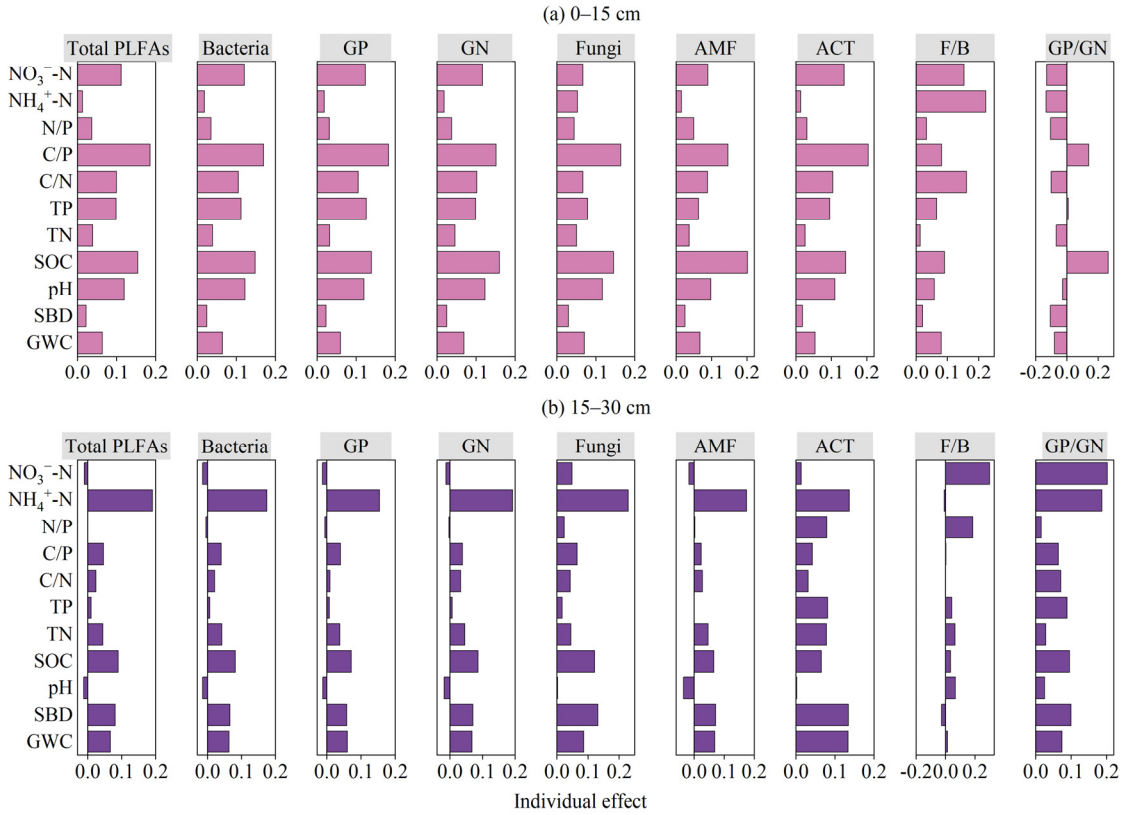

Figure 4. The relative importance of soil physicochemical properties on soil microbial communities was determined for (**a**) 0–15 cm and (**b**) 15–30 cm soil depths using hierarchical partitioning analysis. The individual effect is used to compare the difference in the proportion of response variables explained between explanatory variables (relative importance), and each variable's individual effects (as determined by hierarchical partitioning) are connected to the sum of its unique and total average shared effects (calculated using variation partitioning) [39]. Abbreviations: actinomycetes (ACT), arbuscular mycorrhizal fungi (AMF), Gram-positive bacteria (GP), Gram-negative bacteria (GN), nitrate nitrogen (NO_3^--N), ammonium nitrogen (NH_4^+-N), total phosphorus (TP), total nitrogen (TN), soil organic carbon (SOC), soil bulk density (SBD), and gravimetric water content (GWC). GP/GN, F/B, N/P, C/P, and C/N represent the ratios of Gram-positive bacteria to Gram-negative bacteria, fungi to bacteria, total nitrogen to total phosphorus, organic carbon to total phosphorus, and organic carbon to total nitrogen, respectively.

Based on the results of the relative importance analysis, we selected C/P, SOC, NO_3^--N, NH_4^+-N, pH, SBD, and GWC with the soil microbial biomass and composition for Pearson correlation analysis (Figure S1). Specifically, the total PLFAs and all functional microbial groups such as GP, GN, bacteria, fungi, AMF, and ACT indicated significant positive correlations with GWC, SOC, and C/P ratio, and sharply negative correlations with SBD. In addition, the total PLFAs and all functional microbial groups were significantly positively correlated with NO_3^--N and negatively correlated with pH at the 0–15 cm soil depth, while they were significantly positively correlated with NH_4^+-N at the 15–30 cm soil depth. The F/B ratio showed a significantly negative correlation with GWC, SOC, C/P ratio, and NO_3^--N and a positive correlation with pH at the 0–15 cm soil depth, while it was only significantly negatively correlated with NO_3^--N at the 15–30 cm soil depth. The GP/GN ratio was positively correlated with SBD and negatively correlated with SOC, C/P ratio, and NH_4^+-N at the 15–30 cm soil depth (Figure S1).

4. Discussion

This study tested our first hypothesis that increases in soil microbial biomass with stand age were accompanied by significant changes in microbial community composition (Figure 1), consistent with other studies on the effects of stand age on soil microbial communities [43,44]. These results may be because the increased input of fresh organic matter favored microbial growth with increasing stand age [23,35]. In addition, the community composition was not consistent with the variation of soil microbial biomass with stand age, and soil depth had a significant effect on the stand-age patterns in microbial communities (Figure 1). These may be attributed to the different adaptability and nutrient requirements of each functional microbial community to the environment [1,45].

The microbial biomass in the soil is highly related to its physicochemical properties (Figures 4 and S1), which is consistent with previous findings [19,46]. The biomass of total PLFAs and all functional microbial groups (including B, F, GP, GN, ACT, and AMF) generally increased with forest age and were positively correlated with SOC content and nutrient content at both soil depths, which could be explained by the accumulation of SOC and nutrients (Table S3). Increasing soil fertility accelerated the growth of soil microbes in forest soils, as previously reported by Mendham et al. [47] and Liu et al. [44]. Interestingly, the biomass trends of total PLFAs and all functional microbial groups differed between the two soil depths with increasing forest age (Figure 1a–g). Specifically, at the 0–15 cm soil depth, the biomass of total PLFAs and all functional microbial groups was significantly lower in the 7-year-old stand than in the other four stand ages, which is consistent with the findings of Liu et al. [44]. Lower values of litterfall, organic matter, water holding capacity, and soil moisture were found in the youngest stands compared to the older stands, which led to lower soil microbial biomass [12,48]. Therefore, the biomass of all functional microbial groups also increased rapidly when canopy density, the height of the trees, GWC, SOC concentration, and nutrient concentrations increased significantly from 7- to 13-year-old stands (Tables S2 and S3). In addition, the amounts of fungi in the 13-year-old stand were significantly lower than those of the other three stand ages (24, 33, and 53 years), while the bacterial groups had no significant difference among these four stand ages (Figures 1e and 3a). The reason for this result may be that the bacteria groups have evolved to grow rapidly in response to the availability of their substrates (e.g., easily degradable compounds), whereas fungi grow much slower in an environment with sufficient nutrient availability [49,50]. Wang et al. [21] found that soil microorganisms were sensitive to SOC dynamics with forest age in plantation ecosystems. This assumption was also supported by our result that the biomass of total PLFAs and all functional microbial groups was mainly affected by SOC concentration and C/P ratio at the 0–15 cm soil depth in the context of forest age sequences (Figure 4). The main driver of soil microbial biomass at the 15–30 cm soil depth was NH_4^+-N, unlike at the 0–15 cm soil depth. Ammonium (NH_4^+) is a key N-form in protein synthesis and metabolism in plants and microorganisms [26], so the fierce competition for N nutrients between microorganisms and plants may explain why NH_4^+-N controlled biomass at the 15–30 cm soil depth [51]. Therefore, the biomass trends of total PLFAs and all functional microbial groups at the 15–30 cm soil depth were consistent with the trend of NH_4^+-N concentration, which first increased and then decreased with increasing stand age, peaking in the 33-year-old stand (Figure 1 and Table S3). Moreover, Chinese cedar (Cupressaceae) is a tree that forms symbiotic associations with AMF, and AMF can make important contributions to water and nutrient (especially phosphorus) uptake for plant growth [52,53]. A study by Matsuda et al. showed that AMF is sensitive to soil conditions and varies with root age [54]. Our finding that the biomass of AMF was consistent with the trends of SWC, TN, and TP with stand age also supported the above conclusions (Figure 1f and Table S3).

The composition of the soil microbial community changed significantly with stand age and was strongly associated with some soil properties (Figures 1h,i, 4 and S1). In our study, bacterial groups (GP and GN) dominated the soil microbial community, with ACT and fungi coming in second (Figures 1 and 2), but their survival strategies with

different stand ages remain to be explored. Wardle et al. [55] pointed out that bacteria are linked to soils with high nutrient supply rates and rapid decomposition, whereas fungi are linked to soils with slow decomposition and low nutrient supply rates. Therefore, the F/B ratio increases as nutrients become less available and growth rates decline [56]. In the present study, the 7-year-old stand is an infertile ecosystem with slow plant growth and low nutrient availability, while the 13-year-old stand has fast plant growth and sufficient nutrients (Tables S2 and S3), so the F/B ratio was highest in the 7-year-old stand and lowest in the 13-year-old stand independent of the soil depth. Most studies indicated that pH was the key driver of the relative dominance of fungi and bacteria in soil [19,33,46]. Another explanation for the variation in the F/B ratio with stand age may be that fungi prefer higher pH than bacteria [57]. At both soil depths, the F/B ratio was positively correlated with pH, decreased with decreasing pH, and did not differ significantly from 24- to 53-year-old stands (Figures 1h and S1, Table S3). In addition, Zechmeister-Boltenstern et al. [20] reported that bacteria have higher N demands than fungi. Wang et al. [9] reported that NH_4^+-N indirectly affected the bacterial community composition by influencing NO_3^--N. Those results were also supported by our result that the F/B ratio was mainly influenced by soil mineral nitrogen (e.g., NO_3^--N and NH_4^+-N) (Figures 4 and S1, Table S3). Both the GN and GP prefer plant-derived carbon as a carbon source based on substrate availability, but the GN used more relatively labile plant-derived carbon sources whereas the GP used more recalcitrant carbon sources derived from soil organic matter [58]. At the 0–15 cm soil depth, SOC was an important factor influencing the GP/GN ratio (Figure 4). Therefore, the GP/GN ratio did not differ significantly with increasing stand age at the 0–15 cm soil depth (Figure 1i), suggesting that GP and GN of each stand age may be able to obtain sufficient plant-sourced carbon (litterfall) at this soil depth. Soil mineral nitrogen (e.g., NO_3^--N and NH_4^+-N) was the main factor regulating the GP/GN ratio at the 15–30 cm soil depth (Figure 4). This result could be explained by fast-growing trees extracting nitrogen from the deep soil and the fierce competition between microorganisms and plants for N nutrients [51,59]. The GP bacteria was more resistant to environmental stress than GN bacteria [60], so the GP bacteria could better adapt to NH_4^+-N limitation at the 15–30 cm soil depth. As a result, the GP/GN ratio was the highest in the 13-year-old stand, where the trees were growing at the fastest rate.

The biomass of total PLFAs and all functional microbial groups increased with stand age at both soil depths and was significantly lower at the 15–30 cm soil depth than at the 0–15 cm soil depth, except in the 7-year-old stand (Figure 1a–g). On the one hand, the reason may be that SOC and nutrient concentrations at the 15–30 cm soil depth were significantly lower than those at the 0–15 cm soil depth (Table S3), which limited the growth of microorganisms [61,62]. On the other hand, high values of soil bulk density (SBD) mean lower porosity and therefore less oxygen availability, which in turn affects the soil microbial biomass [63,64]. In our study, SBD was significantly inversely related to all soil microbial biomass (Figure S1), indicating that higher SBD in the 15–30 cm soil depth may limit soil microorganism growth. The F/B ratio did not differ significantly between soil depths. SOC and mineral nitrogen (i.e., NH_4^+-N and NO_3^--N) played a role in regulating the composition of the microbial community (F/B ratio and GP/GN ratio) at both soil depths (Figure 4).

5. Conclusions

Our results indicated that the biomass of total PLFAs and functional microbial groups increased largely with increasing forest age at both soil depths but reached a peak at different forest ages. The biomass of the 0–15 cm soil depth increased significantly from 7- to 13-year-old forests and then stabilized, while the biomass of the 15–30 cm soil depth was the highest in the 33-year-old stand. The 13-year-old stand had a significantly different bacterial and fungal community composition than the remaining four stand ages. The biomass and GP/GN ratio of the 0–15 cm soil depth were adjusted by SOC and C/P ratios, whereas the 15–30 cm soil depth was mainly explained by NH_4^+-N. Furthermore, NO_3^--N

determined the relative dominance of bacteria and fungi at both soil depths. Overall, the soil microbial community recovered rapidly and had a high percentage of bacteria in the early stages of afforestation.

Supplementary Materials: The following supporting information can be downloaded at https://www.mdpi.com/article/10.3390/f14030470/s1, Table S1: Selected basic climate data information of the study area in the last three years (2019–2021); Table S2: The basic information on *Cryptomeria japonica var. sinensis* plantations at different stand ages is from the survey conducted in August 2020; Table S3: Soil physicochemical properties for each stand age in July 2021; Table S4: *p* value and F value based on a two-way ANOVA for the proportion of functional groups; Figure S1: Correlation analysis of the soil microbial biomass and composition with selected soil physicochemical properties.

Author Contributions: Conceptualization, Y.S. and Z.X.; Data curation, Y.S., S.X. and Y.L.; Formal analysis, Y.S. and S.X.; Funding acquisition, Z.X.; Investigation, S.X., Y.L., Z.H. and J.L.; Methodology, C.Y., B.T. and Z.X.; Project administration, C.Y., B.T. and Z.X.; Resources, B.T. and Z.X.; Software, Y.S., Y.H., L.W. and S.L.; Supervision, C.Y., B.T. and Z.X.; Validation, S.X., C.Y. and Z.H.; Visualization, Y.S., S.X., C.Y., B.T. and Z.X.; Writing–original draft, Y.S.; Writing—review and editing, Y.S., C.Y., L.Z., H.L., B.T. and Z.X. All authors have read and agreed to the published version of the manuscript.

Funding: This work was supported by the National Natural Science Foundation of China (32071745, 31870602, and 31901295), the Program of Sichuan Excellent Youth Sci-Tech Foundation (2020JDJQ0052), the Program of Sichuan Applied Basic Research Foundation (2022NSFSC0997, 2021YJ0340), and the National Key Research and Development Program of China (2017YFC0505003).

Data Availability Statement: Not applicable.

Acknowledgments: We would like to thank the Key Laboratory of Vegetation Restoration and Management of Degraded Ecosystems & CAS Engineering Laboratory for Vegetation Ecosystem Restoration on Islands and Coastal Zones, South China Botanical Garden, Chinese Academy of Sciences for their support in processing our phospholipid fatty acid (PLFA) analysis. We would also like to thank Jiangshan Lai for his kind help with PERMANOVA and hierarchical partitioning analysis.

Conflicts of Interest: The authors declare no conflict of interest.

References

1. Bahram, M.; Hildebrand, F.; Forslund, S.K.; Anderson, J.L.; Soudzilovskaia, N.A.; Bodegom, P.M.; Bengtsson-Palme, J.; Anslan, S.; Coelho, L.P.; Harend, H.; et al. Structure and function of the global topsoil microbiome. *Nature* **2018**, *560*, 233–237. [CrossRef] [PubMed]
2. Smith, A.P.; Marín-Spiotta, E.; Balser, T. Successional and seasonal variations in soil and litter microbial community structure and function during tropical postagricultural forest regeneration: A multiyear study. *Glob. Chang. Biol.* **2015**, *21*, 3532–3547. [CrossRef]
3. van der Heijden, M.G.A.; Bardgett, R.D.; van Straalen, N.M. The unseen majority: Soil microbes as drivers of plant diversity and productivity in terrestrial ecosystems. *Ecol. Lett.* **2008**, *11*, 296–310. [CrossRef]
4. Schloter, M.; Dilly, O.; Munch, J.C. Indicators for evaluating soil quality. *Agric. Ecosyst. Environ.* **2003**, *98*, 255–262. [CrossRef]
5. Jing, Y.; Tian, P.; Wang, Q.; Li, W.; Sun, Z.; Yang, H. Effects of root dominate over aboveground litter on soil microbial biomass in global forest ecosystems. *For. Ecosyst.* **2021**, *8*, 38. [CrossRef]
6. Steidinger, B.S.; Crowther, T.W.; Liang, J.; Van Nuland, M.E.; Werner, G.D.A.; Reich, P.B.; Nabuurs, G.J.; De-Miguel, S.; Zhou, M.; Picard, N.; et al. Climatic controls of decomposition drive the global biogeography of forest-tree symbioses. *Nature* **2019**, *569*, 404–408. [CrossRef]
7. FAO. Global Forest Resources Assessment 2015: How Are the World's Forests Changing? Available online: https://www.fao.org/forest-resources-assessment/2020/en/ (accessed on 15 October 2022).
8. Yang, K.; Diao, M.; Zhu, J.; Lu, D.; Zhang, W. A global meta-analysis of indicators for assessing forest soil quality through comparison between paired plantationsversus natural forests. *Land Degrad. Dev.* **2022**, *33*, 3603–3616. [CrossRef]
9. Wang, Y.; Jiao, P.; Guo, W.; Du, D.; Hu, Y.; Tan, X.; Liu, X. Changes in bulk and rhizosphere soil microbial diversity and composition along an age gradient of Chinese Fir (*Cunninghamia lanceolate*) plantations in subtropical China. *Front. Microbiol.* **2022**, *12*, 777862. [CrossRef] [PubMed]
10. Xu, M.; Lu, X.; Xu, Y.; Zhong, Z.; Zhang, W.; Ren, C.; Han, X.; Yang, G.; Feng, Y. Dynamics of bacterial community in litter and soil along a chronosequence of *Robinia pseudoacacia* plantations. *Sci. Total Environ.* **2020**, *703*, 135613. [CrossRef]
11. Jourgholami, M.; Ghassemi, T.; Labelle, E.R. Soil physio-chemical and biological indicators to evaluate the restoration of compacted soil following reforestation. *Ecol. Indic.* **2019**, *101*, 102–110. [CrossRef]

12. Lucas-Borja, M.E.; Hedo, J.; Cerdá, A.; Candel-Pérez, D.; Viñegla, B. Unravelling the importance of forest age stand and forest structure driving microbiological soil properties, enzymatic activities and soil nutrients content in Mediterranean Spanish black pine (*Pinus nigra Ar.* ssp. *salzmannii*) Forest. *Sci. Total Environ.* **2016**, *562*, 145–154. [CrossRef] [PubMed]
13. Richter, A.; Schöning, I.; Kahl, T.; Bauhus, J.; Ruess, L. Regional environmental conditions shape microbial community structure stronger than local forest management intensity. *For. Ecol. Manag.* **2018**, *409*, 250–259. [CrossRef]
14. Wu, H.; Xiang, W.; Ouyang, S.; Xiao, W.; Li, S.; Chen, L.; Lei, P.; Deng, X.; Zeng, Y.; Zeng, L.; et al. Tree growth rate and soil nutrient status determine the shift in nutrient-use strategy of Chinese fir plantations along a chronosequence. *For. Ecol. Manag.* **2020**, *460*, 117896. [CrossRef]
15. Lauber, C.L.; Strickland, M.S.; Bradford, M.A.; Fierer, N. The influence of soil properties on the structure of bacterial and fungal communities across land-use types. *Soil Biol. Biochem.* **2008**, *40*, 2407–2415. [CrossRef]
16. Linn, D.M.; Doran, J.W. Effect of water-filled pore space on carbon dioxide and nitrous oxide production in tilled and nontilled soils. *Soil Sci. Soc. Am. J.* **1984**, *48*, 1267–1272. [CrossRef]
17. Ebrahimi, A.; Or, D. Microbial community dynamics in soil aggregates shape biogeochemical gas fluxes from soil profiles—Upscaling an aggregate biophysical model. *Glob. Chang. Biol.* **2016**, *22*, 3141–3156. [CrossRef]
18. Bååth, E.; Anderson, T.H. Comparison of soil fungal/bacterial ratios in a pH gradient using physiological and PLFA-based techniques. *Soil Biol. Biochem.* **2003**, *35*, 955–963. [CrossRef]
19. Li, Q.; Feng, J.; Wu, J.; Jia, W.; Zhang, Q.; Chen, Q.; Zhang, D.; Cheng, X. Spatial variation in soil microbial community structure and its relation to plant distribution and local environments following afforestation in central China. *Soil Tillage Res.* **2019**, *193*, 8–16. [CrossRef]
20. Zechmeister-Boltenstern, S.; Keiblinger, K.M.; Mooshammer, M.; Peñuelas, J.; Richter, A.; Sardans, J.; Wanek, W. The application of ecological stoichiometry to plant-microbial-soil organic matter transformations. *Ecol. Monogr.* **2015**, *85*, 133–155. [CrossRef]
21. Wang, C.; Xue, L.; Jiao, R. Soil organic carbon fractions, C-cycling associated hydrolytic enzymes, and microbial carbon metabolism vary with stand age in *Cunninghamia lanceolate* (Lamb.) Hook plantations. *For. Ecol. Manag.* **2021**, *482*, 118887. [CrossRef]
22. Xia, Q.; Chen, L.; Xiang, W.; Ouyang, S.; Wu, H.; Lei, P.; Xiao, W.; Li, S.; Zeng, L.; Kuzyakov, Y. Increase of soil nitrogen availability and recycling with stand age of Chinese-fir plantations. *For. Ecol. Manag.* **2021**, *480*, 118643. [CrossRef]
23. Nouvellon, Y.; Epron, D.; Marsden, C.; Kinana, A.; Le Maire, G.; Deleporte, P.; Saint-André, L.; Bouillet, J.; Laclau, J. Age-related changes in litter inputs explain annual trends in soil CO_2 effluxes over a full *Eucalyptus* rotation after afforestation of a tropical savannah. *Biogeochemistry* **2012**, *111*, 515–533. [CrossRef]
24. Wang, J.; Liu, J.; Huang, Y.; Yang, J. The origin and natural distribution of *Cryptomeria*. *J Sichuan For. Sci. Technol.* **2007**, *28*, 92–94. [CrossRef]
25. Gong, Y.; Wang, R.; Zhang, B.; Liu, K.; Dong, K. Effects of thinning on growth and soil organic carbon of *Cryptomeria fortunei* Plantation in Western Sichuan. *For. Resour Manag.* **2020**, *6*, 96–104. [CrossRef]
26. Templer, P.H.; Silver, W.L.; Pett-Ridge, J.; M DeAngelis, D.K.; Firestone, M.K. Plant and microbial controls on nitrogen retention and loss in a humid tropical forest. *Ecology* **2008**, *89*, 3030–3040. [CrossRef]
27. Liu, X.; Cui, N.; Tan, F.; Hong, Z.; Xiong, S.; Meng, Y.; Tan, B.; Li, H.; Xu, Z.; Zhang, J.; et al. The soil water holding capacity and its indicative effect on soil organic carbon of *Cryptomeria japonica* plantations in the rainy area of western China. *Chin. J. Appl. Environ. Biol.* **2022**. [CrossRef]
28. Robertson, G.P.; Coleman, D.C.; Bledsoe, C.S.; Sollins, P. *Standard Soil Methods for Long-Term Ecological Research*, 2nd ed.; Oxford University Press: New York, NY, USA, 1999; pp. 55–182.
29. He, X.; Huang, Y.; Zhang, Q.; Ye, S.; Wang, S. Distribution of organic carbon fractions in soil aggregates in Chinese fir plantations with different stand ages. *Ecol. Process.* **2021**, *10*, 49. [CrossRef]
30. Buyer, J.S.; Sasser, M. High throughput phospholipid fatty acid analysis of soils. *Appl. Soil Ecol.* **2012**, *61*, 127–130. [CrossRef]
31. Frostegård, A.; Bååth, E. The use of phospholipid fatty acid analysis to estimate bacterial and fungal biomass in soil. *Biol. Fertil. Soils* **1996**, *22*, 59–65. [CrossRef]
32. Fanin, N.; Kardol, P.; Farrell, M.; Nilsson, M.; Gundale, M.J.; Wardle, D.A. The ratio of Gram-positive to Gram-negative bacterial PLFA markers as an indicator of carbon availability in organic soils. *Soil Biol. Biochem.* **2019**, *128*, 111–114. [CrossRef]
33. Frostegård, Å.; Bååth, E.; Tunlio, A. Shifts in the structure of soil microbial communities in limed forests as revealed by phospholipid fatty acid analysis. *Soil Biol. Biochem.* **1993**, *25*, 723–730. [CrossRef]
34. Zogg, G.P.; Zak, D.R.; Ringelberg, D.B.; White, D.C.; Macdonald, N.W.; Pregitzer, K.S. Compositional and functional shifts in microbial communities due to soil warming. *Soil Sci. Soc. Am. J.* **1997**, *61*, 475–481. [CrossRef]
35. Wang, H.; Boutton, T.W.; Xu, W.; Hu, G.; Jiang, P.; Bai, E. Quality of fresh organic matter affects priming of soil organic matter and substrate utilization patterns of microbes. *Sci. Rep.* **2015**, *5*, 10102. [CrossRef] [PubMed]
36. Hill, G.T.; Mitkowski, N.A.; Aldrich-Wolfe, L.; Emele, L.R.; Jurkonie, D.D.; Ficke, A.; Maldonado-Ramirez, S.; Lynch, S.T.; Nelson, E.B. Methods for assessing the composition and diversity of soil microbial communities. *Appl. Soil Ecol.* **2000**, *15*, 25–36. [CrossRef]
37. Ruess, L.; Chamberlain, P.M. The fat that matters: Soil food web analysis using fatty acids and their carbon stable isotope signature. *Soil Biol. Biochem.* **2010**, *42*, 1898–1910. [CrossRef]
38. Bossio, D.A.; Fleck, J.A.; Scow, K.M.; Fujii, R. Alteration of soil microbial communities and water quality in restored wetlands. *Soil Biol. Biochem.* **2006**, *38*, 1223–1233. [CrossRef]

39. Lai, J.; Zou, Y.; Zhang, J.; Peres Neto, P.R. Generalizing hierarchical and variation partitioning in multiple regression and canonical analyses using the rdacca.hp R package. *Methods Ecol. Evol.* **2022**, *13*, 782–788. [CrossRef]
40. Oksanen, J.; Simpson, G.L.; Blanchet, F.G.; Kindt, R.; Legendre, P.; Minchin, P.R.; O'Hara, R.B.; Solymos, P. Vegan: Community Ecology Package. R Package Version 2.6-2. Available online: https://CRAN.R-project.org/package=vegan (accessed on 25 June 2022).
41. Wickham, H. *ggplot2: Elegant Graphics for Data Analysis*; Springer: New York, NY, USA, 2016.
42. Schloerke, B.; Cook, D.; Larmarange, J.; Briatte, F.; Marbach, M.; Thoen, E.; Elberg, A.; Crowley, J. GGally: Extension to 'ggplot2'. Available online: https://CRAN.R-project.org/package=GGally (accessed on 1 December 2022).
43. Wu, X.; Xu, H.; Tuo, D.; Wang, C.; Fu, B.; Lv, Y.; Liu, G. Land use change and stand age regulate soil respiration by influencing soil substrate supply and microbial community. *Geoderma* **2020**, *359*, 113991. [CrossRef]
44. Liu, D.; Huang, Y.; Sun, H.; An, S. The restoration age of *Robinia pseudoacacia* plantation impacts soil microbial biomass and microbial community structure in the Loess Plateau. *Catena* **2018**, *165*, 192–200. [CrossRef]
45. Shanmugam, S.G.; Kingery, W.L. Changes in soil microbial community structure in relation to plant succession and soil properties during 4000 years of pedogenesis. *Eur. J. Soil Biol.* **2018**, *88*, 80–88. [CrossRef]
46. de Vries, F.T.; Manning, P.; Tallowin, J.R.B.; Mortimer, S.R.; Pilgrim, E.S.; Harrison, K.A.; Hobbs, P.J.; Quirk, H.; Shipley, B.; Cornelissen, J.H.C.; et al. Abiotic drivers and plant traits explain landscape-scale patterns in soil microbial communities. *Ecol. Lett.* **2012**, *15*, 1230–1239. [CrossRef] [PubMed]
47. Mendham, D. Eucalyptus globulus harvest residue management effects on soil carbon and microbial biomass at 1 and 5 years after plantation establishment. *Soil Biol. Biochem.* **2002**, *34*, 1903–1912. [CrossRef]
48. Teklay, T.; Shi, Z.; Attaeian, B.; Chang, S.X. Temperature and substrate effects on C & N mineralization and microbial community function of soils from a hybrid poplar chronosequence. *Appl. Soil Ecol.* **2010**, *46*, 413–421. [CrossRef]
49. Ingwersen, J.; Poll, C.; Streck, T.; Kandeler, E. Micro-scale modelling of carbon turnover driven by microbial succession at a biogeochemical interface. *Soil Biol. Biochem.* **2008**, *40*, 864–878. [CrossRef]
50. Blagodatskaya, E.V.; Anderson, T. Interactive effects of pH and substrate quality on the fungal-to-bacterial ratio and QCO_2 of microbial communities in forest soils. *Soil Biol. Biochem.* **1998**, *30*, 1269–1274. [CrossRef]
51. Geisseler, D.; Horwath, W.R.; Joergensen, R.G.; Ludwig, B. Pathways of nitrogen utilization by soil microorganisms-A review. *Soil Biol. Biochem.* **2010**, *42*, 2058–2067. [CrossRef]
52. Smith, S.E.; Read, D. *Mycorrhizal Symbiosis*, 3rd ed.; Academic Press is an Imprint of Elsevier: London, UK, 2008; pp. 11–188.
53. Lanfranco, L.; Bonfante, P. The need for phosphate: At the root of the mycorrhizal symbiosis. *Sci. Bull.* **2022**, *67*, 459–460. [CrossRef]
54. Matsuda, Y.; Kita, K.; Kitagami, Y.; Tanikawa, T. Colonization status and community structure of arbuscular mycorrhizal fungi in the coniferous tree, *Cryptomeria japonica*, with special reference to root orders. *Plant Soil* **2021**, *468*, 423–438. [CrossRef]
55. Wardle, D.A.; Bardgett, R.D.; Klironomos, J.N.; Setala, H.; van der Putten, W.H.; Wall, D.H. Ecological linkages between aboveground and belowground biota. *Science* **2004**, *304*, 1629–1633. [CrossRef]
56. Orwin, K.H.; Dickie, I.A.; Holdaway, R.; Wood, J.R. A comparison of the ability of PLFA and 16S rRNA gene metabarcoding to resolve soil community change and predict ecosystem functions. *Soil Biol. Biochem.* **2018**, *117*, 27–35. [CrossRef]
57. Iovieno, P.; Alfani, A.; Bååth, E. Soil microbial community structure and biomass as affected by *Pinus pinea* plantation in two Mediterranean areas. *Appl. Soil Ecol.* **2010**, *45*, 56–63. [CrossRef]
58. Kramer, C.; Gleixner, G. Soil organic matter in soil depth profiles: Distinct carbon preferences of microbial groups during carbon transformation. *Soil Biol. Biochem.* **2008**, *40*, 425–433. [CrossRef]
59. Gao, X.; Li, X.G.; Zhao, L.; Kuzyakov, Y. Regulation of soil phosphorus cycling in grasslands by shrubs. *Soil Biol. Biochem.* **2019**, *133*, 1–11. [CrossRef]
60. Moore-Kucera, J.; Dick, R.P. PLFA profiling of microbial community structure and seasonal shifts in soils of a Douglas-fir Chronosequence. *Microb. Ecol.* **2008**, *55*, 500–511. [CrossRef]
61. Fierer, N.; Schimel, J.P.; Holden, P.A. Variations in microbial community composition through two soil depth profiles. *Soil Biol. Biochem.* **2003**, *35*, 167–176. [CrossRef]
62. Hu, L.; Ade, L.; Wu, X.; Zi, H.; Luo, X.; Wang, C. Changes in soil C:N:P stoichiometry and microbial structure along soil depth in two forest soils. *Forests* **2019**, *10*, 113. [CrossRef]
63. Ebrahimi, A.; Or, D. Hydration and diffusion processes shape microbial community organization and function in model soil aggregates. *Water Resour. Res.* **2015**, *51*, 9804–9827. [CrossRef]
64. Meyer, C.; Lüscher, P.; Schulin, R. Enhancing the regeneration of compacted forest soils by planting black alder in skid lane tracks. *Eur. J. For. Res.* **2014**, *133*, 453–465. [CrossRef]